AUTOMATIC HISTOLOGICAL CLASSIFICATION OF COLON CANCER USING COMBINED TEXTURAL AND MORPHOLOGICAL PARAMETERS

K.A. MARGHANI*#, S.S. DLAY**, B.S. SHARIF**, A.J. SIMS***, A.O. ELHMASSI*, A.M. ELHAJ*

*Department of Physics, Faculty of Science, University of Tripoli, Tripoli, Libya, #e-mail:
k.marghani@uot.edu.ly
**School of Electrical, Electronic and Computer Eng., University of Newcastle upon Tyne,
Newcastle upon Tyne, NE1 7RU, UK
***Regional Medical Physics Department, Freeman Hospital, Newcastle upon Tyne, NE7 7DN, UK

Abstract. A new automated algorithm for accurate and reliable decision-making in the discrimination of normal and cancerous colon mucosa is proposed. Quantitative texture features such as entropy, angular second moment, contrast, inverse angular moment, correlation, homogeneity, were extracted from the co-occurrence matrix whilst other features are based on morphology such as Euler number, convex area, nuclear contour index, elongation, shape factor (BE) and fractal dimension. 46 samples from different patients consisting of 22 normal microscopic specimens and 24 adenocarcinoma images ($512\times512\times3$) were analyzed. Extracted features from both dimensions were able to identify abnormalities ($P < 0.0001$) between colon tissue types. A parametric approach using a linear discrimination method was implemented for the classification stage. Combining texture and morphological features shows that a ratio of 98.3 % and 97.7 % is obtained for the sensitivity and specificity, respectively. Only one case from each class was wrongly misclassified. The proposed algorithm achieves a very significant result with an overall accuracy of 98 % for the identification of colon microscopic images.

Key words: Image analysis, colon tissue, medical diagnosis, quantitative measurements, morphology, texture, shape, histology, linear discrimination, cancer diagnosis.

INTRODUCTION

Numerous studies have aimed at developing image analysis procedures for the resolution of difficult differential diagnoses in cytology and histopathology, particularly since manual examination of tissue has been shown to be time consuming and subject to sampling error. However, the applications of quantitative analysis in medical diagnosis of certain types of cancers remain limited due to the complexity of the microscopic images in terms of their shape and configuration [16].

A number of quantitative approaches have been suggested [3, 4, 6, 9, 10, 15, 16, 27, 29, 32]. Two different approaches, known as texture and morphology for the classification of images of normal and malignant tissues, are investigated in this paper due to their success in other cancer diagnosis applications [2, 11, 12, 16, 17, 18, 23, 35]. Features derived from morphometric approaches can lead to remarkable results in the analysis of histological examination [16]. Hamilton *et al.* [17] used semi-automatic image analysis to undertake a morphometrical assessment in order to quantify the descriptive differences between normal and malignant colorectal epithelium. Aziz [2] pointed out that histopathological features such as nuclear size, shape, and pleomorphism must be converted to image features such as area, shape factor, and area variance; this feature vector must be correlated with the pathologist's expert opinion or diagnosis. Thiran [35] has proposed more advanced method for automatic recognition of microscopic cancer images, where he pointed out that mathematical morphology provides good efficiency for the purpose of classification of digital cancer images. Previously published [3], and our previously results [23] showed significant result for the classification of histological images using morphological analysis based on the shape and structure. The most common features used in practice are those derived from the grey level co-occurrence matrix (GLCM) [7, 19]. A review of many different texture features was present in [5, 20, 22]. Hamilton *et al.* [18] used texture features, based on the co-occurrence matrix, and also investigated the number of low optical density pixels in the image, to classify colon cancer. Similar results using texture features had obtained in [11, 30, 31]. Esgiar *et al.* [12] have shown further progress in classifying abnormalities in colon cancer when they accompanied fractal dimension (FD) with both correlation and entropy texture features. Combined wavelet, Local binary pattern LBP and Gaber wavelet texture features [22] showed an accuracy of 88.38 % on the grade of histological tissues of oral sub-mucous fibrosis. Color texture analysis has also been investigated [36] for the discrimination analysis of colon mucosa tissues. As expected, better results of 97.1 % accuracy level using color descriptors were reached compared with 94.4 % with grey level images to identify abnormalities. In another study reported in [24], it was claimed that combining low frequency texture measurements of multiresolution color texture with fine texture measurements could show a significant improvement to 99.4 % accuracy. In contrast, several feature extraction algorithms' based on texture were later presented [28] and then a comparison between two different classification algorithms, known as genetic algorithm and artificial neural network were implemented [1]. The aim of this study is, first, to consider GLCM for the identification of histological images of colon tissue using normalized dataset, and second to investigate a novel approach of combining measurements for comparison with the previous work using parametric linear discrimination method. In this work, different approaches based on texture and morphology analysis to describe the structure of microscopic colonic tissues were examined. Significant differences in selected features between normal and malignant cases were identified using texture in conjunction with morphology. A novel

approach of combining texture and morphological approaches shows a significant improvement in the discrimination between normal and cancerous colon dataset.

MATERIALS AND METHODS

MEDICAL PREPARATION AND SAMPLE COLLECTION

Image acquisition

All samples of freshly received biopsies after resection were fixed with small plastic cassette in formalin. After a period of 24-hour, samples were placed into fixative for a further 24 hours. Next, all samples were sliced thinly (3~4 mm) because, penetration into a thin section will occur more rapidly than for thick sections. Slices were implanted in paraffin, which is comparable in density to tissue, and were sectioned between 3 and 8 μm. Samples were finally, immunohistochemically stained for cytokeratins to enable tissue configuration and regions to be identified. All slide images were digitally acquired using a light microscope (under low magnification of ×40) and JVC CCD camera (Victor Company of Japan Ltd., Yokohama, Japan) attached to a Leica Q500c image analysis system. The images were sampled and digitized in 8-bit format with grey level range 0−255, and were finally stored in 512×512 size formats. A total of 46 cases from two different colon tissue types were digitally acquired composing 24 microscopic image samples representing moderately differentiated adenocarcinoma samples, and 22 image samples of normal colon tissues.

Image sampling

To overcome image-processing problems associated with images that do not contain enough tissue, images were rescaled. All images were divided into four small images (regions) of size 256×256. Each new image was subjected to automatic thresholding based on the local variance using Visilog (Noesis) image processing software by defining the variance of the grey levels above and below the threshold. By minimizing the sum of two variances, the threshold level was defined. Regions with more than 90 % of pixels below the threshold level were rejected. Finally, 102 samples (21.66×21.66 mm size) from 184 original images, representing 44 cases of normal tissues and 58 of malignant image samples, were selected and used for examinations. The selection was based on the texture, independent of the patient's number, and therefore the rejection rate was high. An example for both cases is illustrated in Figure 1. The data could be improved if it is calibrated and subjected to a gamma-correcting function, although some filters have been applied to remove noise.
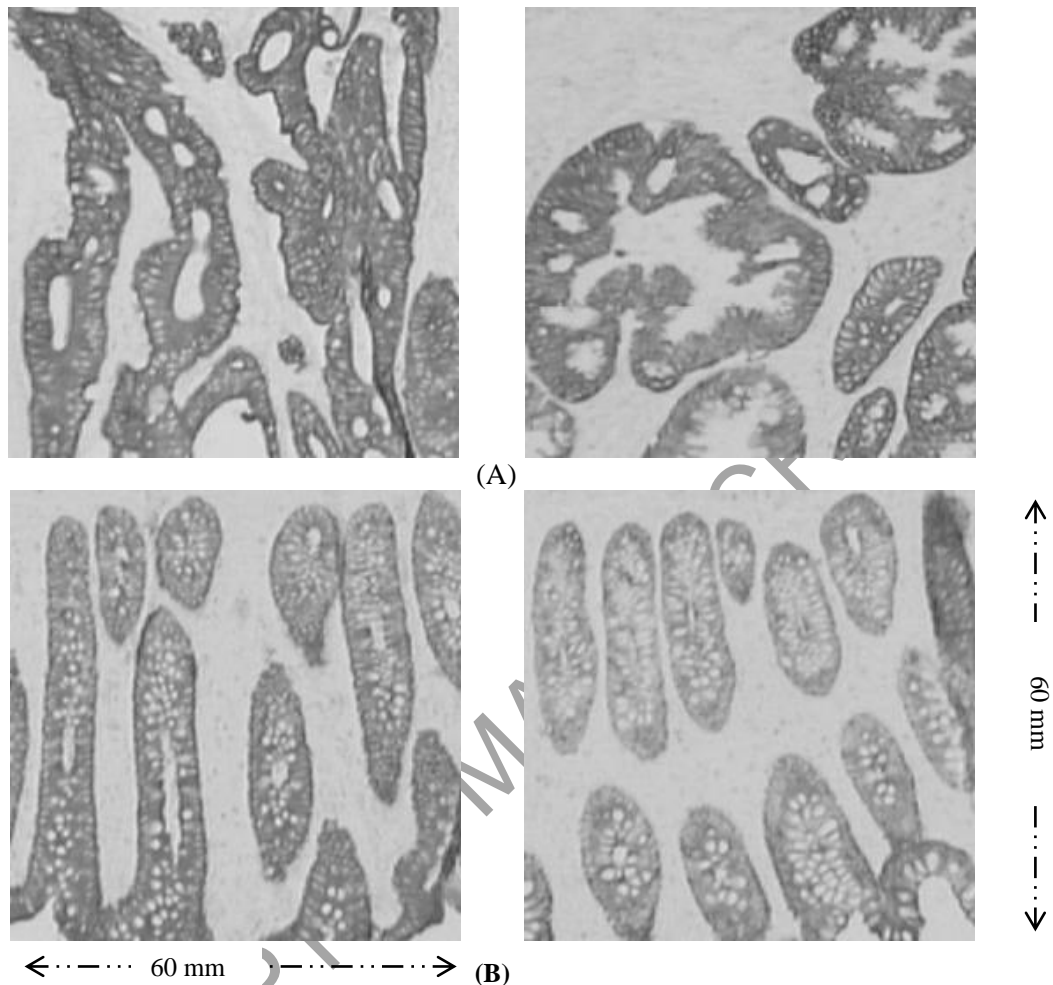
Fig. 1. Examples set of two types of colon tissues ($\times$ 40) in 2D gray-level digital image format (256$\times$256 pixel size): (A) cancer tissue images, (B) normal sample images.

FEATURE EXTRACTION METHODS

The discrimination between normal colorectal glands and moderately differentiated adenocarcinoma was based on features extracted by using two different classes of descriptors. The first considered the grey level changes using the co-occurrence matrix method, and the most important corresponding texture features of the normalized dataset were estimated. The second method used a morphological approach based on the shape and structure of the gland objects of a previously published dataset [23].

Texture feature extraction

The GLCM method was used in order to transform image information into quantitative measurements representing the texture features. This method was extensively studied and implemented for different applications and has been suggested as one of the best texture analysis approaches [5, 7, 19, 20, 22, 25]. Texture can be qualitatively described as being fine or coarse, grainy or smooth, random or regular, linear or mottled, having certain directionality. In order to quantify visual sense into quantitative measurements, six second-order statistical texture features, were extracted [19]. These were entropy, angular second moment (ASM), contrast, inverse difference moment (INVDM), correlation, and homogeneity. Each of which has a special property that partially describes the grey level characterization. For computational convenience, all images were linearly rescaled to 32 grey levels. This was to ensure that the major changes of the grey levels values were captured by the GLCM to improve the statistical validity. Figure (4b) and (4d) shows an example of the rescaled images. Each 256×256 pixel size image was divided into 13×13 non overlapping windows, of size 19×19 pixels each. For window size $M \times N$ and distance $d = 1$ pixel in the horizontal direction, the co-occurrence matrix P is defined as follows:

$$P(i, j, d = 1, \theta = 0^o) = \# \{(k, l), (m, n) \in \phi, |k - m| = 0, |l - n| =$$
$$= d, I(k, l) = i, I(m, n) = j\} \tag{1}$$

$$P(i, j, d = 1, \theta = 45^o) = \# \{(k, l), (m, n) \in \phi, ((k - m) = d, (l - n)d)$$
$$\text{or} ((k - m) = -d, (l - n) = d), I(k, l) = i, I(m, n) = j) \ \} \tag{2}$$

$$P(i, j, d = 1, \theta = 90^o) = \# \{ (k, l), (m, n) \in \phi, |k - m| - d, |l - n| =$$
$$0, I(k, l) = i, I(m, n) = j\} \tag{3}$$

$$P(i, j, d = 1, \theta = 135^o) = \# \{(k, l), (m, n) \in \phi, ((k - m) = d, (l - n)d)$$
$$\text{or} ((k - m) = -d, (l - n) = -d), I(k, l) = i, I(m, n) = j \ \} \tag{4}$$

where $i, j = 0 \ldots 31$ (number of possible gray-levels), $k, m = 1 \ldots M$ (image width), $l, n = 1 \ldots N$ (image height). Also, ϕ is a finite trace $S = M \times N$ over the image I, and defined as: $\phi = \{(k, l, (m, n): \ 1 \leq (k, l), (m, n \leq S))\}$.

Using the above equation for each direction of θ of 0, 45, 90, 135 degrees, and their transpose, GLCMs were calculated for every small window of the image. This produced symmetrical matrices with pixels identical around the diagonal. The GLCM (P) was normalized, after calculating all directions, to describe the probability of how many times the specific outcome number occurs. Only windows containing enough tissue (more than 25 %) were used for further processing. Then,

from the GLCM, the statistical texture parameters (Table 1) were estimated four times for each image to present all directions (169×4 for images containing enough tissue). Finally, an average value for each feature was calculated (Table 2).

Table 1

Definition of GLCM textural features for 2-D images

Feature	Definition
Normalization matrix	$$P(i,j) = \frac{P(i,j)}{\sum\sum P(i,j)}$$
Marginal-probability matrices	
Row sum	$$P_x(i) = \sum_j P(i,j)$$
Column sum	$$P_x(i) = \sum_i P(i,j)$$
Texture feature	
Entropy	$$F_1 = -\sum_i\sum_j P(i,j)\log P(i,j)$$
Angular second moment	$$F_2 \sum_{i\,j} P(i,j)^2$$
Contrast	$$F_3 = \sum_i\sum_j (i-j)^2\, P(i,j)$$
Inverse difference moment	$$F_4 = \sum_i\sum_j \frac{P(i,j)}{1+(i-j)^2}$$
Correlation	$$F_5\ \frac{\sum_i\sum_j (i,j)P(i,j) - \mu_x\,\mu_y}{\sigma_x\,\sigma_y}$$
Homogeneity	$$F_6 = \sum_i\sum_j \frac{P(i,j)}{1+|(i-j)|}$$

Where the $\mu_x\ \mu_y$ and $\sigma_x\ \sigma_y$ are the mean and the standard deviation of P_x and P_y.

Table 2

Statistical evaluation in comparison between normal and colon cancer tissue type for the texture
feature estimated (Mean ± standard deviation) with t-test.

Texture feature	Normal	Malignant	*P* values
Entropy	3.3232±0.2229	3.0354±0.1900	*P* < 0.0001
Angular second mom	0.1625±0.0268	0.2004±0.0273	*P* < 0.0001
Contrast	0.5519±0.0984	0.4586±0.0716	*P* < 0.0001
Inverse differences moment	0.7901±0.0232	0.8158±0.0188	*P* < 0.0001
Correlation	0.6523±0.1011	0.8122±0.1460	*P* < 0.0001
Homogeneity	25.624±6.196	20.957±4.4144	*P* < 0.0001

Morphological feature extraction

One of the main techniques in quantitative microscopy is image segmentation and feature extraction using morphometric measurements. Methods based on morphometry give quantitative description of structure, and in general, provide measurements of geometric cell and tissue features [25]. On the other hand, manual methods of the evaluation of the tissue sections with dimension reduction are generally based on the principle of geometrical probability using microscopic eyepiece. This technique is not routinely performed since it is time consuming. Therefore, several approaches of using quantitative measurements based on morphology were reported [32].

Feature extraction based morphology is mainly subject to a successful segmentation of the region of interest. 2D grey level images of colon tissues were obtained for processing to separate regions of corresponding interest. However, this is not an easy task due to the complexity inherited of microscopic images. Therefore, samples were segmented using thresholding method [1, 34] that chooses the threshold to minimize the interclass variance of the black and white pixels. Figure (2) shows the original colon sample (a) and its segmented form (b). Images were then subjected to morphological image processing operations such as filling, dilation and erosion suggested by [32, 33]. Firstly, a hole-filling process was applied, where the image was filtered using the opening operation with disk element that removed superfluous overlapped objects. Then, dilation has applied with a small square structure element of size (3×3) to recover any loss of the original shape. Finally, an opening operation was applied for the second time to ensure that tissue objects were separated and the final segmented form can be seen in Figure 2(c).

(A)   (B)
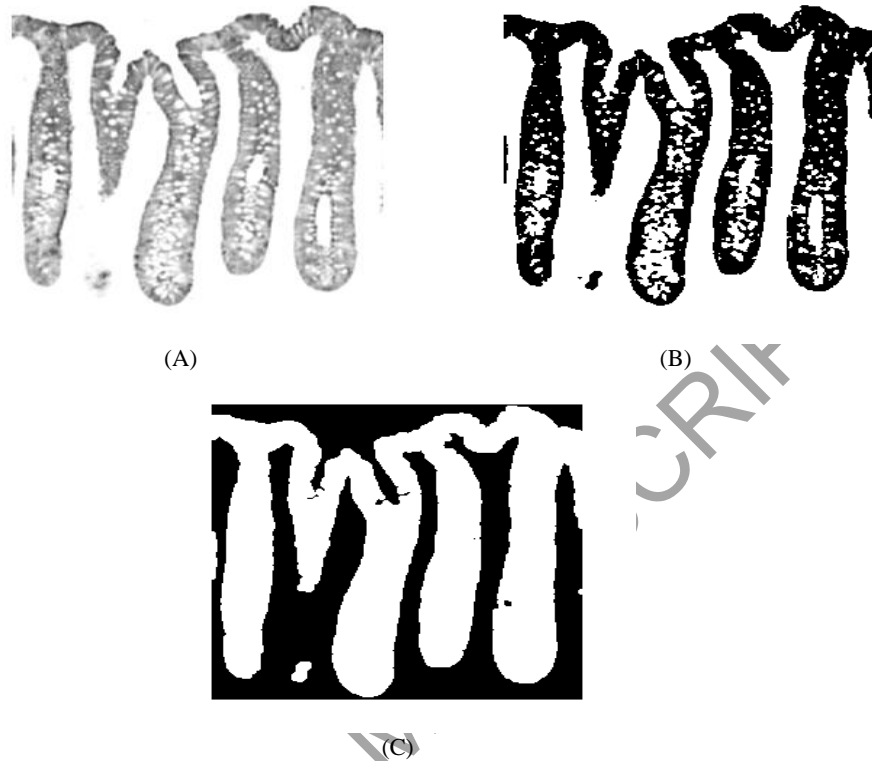
(C)

Fig. 2. Colon normal image; (A) Normal image presenting regular shape and the glands object are distributed in regular form; (B) thresholds image; (C) segmented image after open/close morphology operations.

In this paper, a set of two-dimensional phase parameters derived from morphological segmentation were examined for the discrimination between normal and malignant colon tissue. Extracted features based on morphology were Euler number, equivalent diameter, convex area, nuclear counter index (NCI), elongation, and the shape factor BE (thinness ratio). These parameters describe the most visual texture characteristics of the objects of foreground images such as the number of closed curves the object includes, the ratio between the major/minor axes, and roundness the object.

Brief descriptions of measured parameters [16] are given as follows:

- Euler number can be defined as the difference between the number of objects and the number of holes contained.
- Convex area is calculated as the area of the convexed object confined to convex polygon that contains the region of interest.
- Elongation, expressed as the ratio between the major to minor axis, gives an elongated as:

$$Elongation = (Major\ Axis\ /\ Minor\ Axis \tag{5}$$

- Nuclear contour index, which is calculated as:

$$NCI = (Perimeter\ /\ (Area)^{1/2}\ ) \tag{6}$$

- Shape factor (BE), also known as thinness ratio and is = (1/*contour ratio*).

$$Ff_{BE} = \frac{4\ \pi\ \times Area}{(Perimeter)^2} \tag{7}$$

The closer the factor to 1, the more circular the object is.

FEATURE SELECTION AND ANALYSIS

Two quantitative features sets were identified in this work. The first corresponds to the statistical texture features while the latter is based on texture morphology. Our main consideration was segmentation and feature extraction for categorization, and subsequently, classification. Therefore, the feature selection approach considers the relative frequency distribution for each group separately. These descriptive examinations were carried out for every single feature in order to specify the differences and significance using the statistical mean, standard deviation, and the Student's t-test. Quantitative features, whose mean values were statistically different, were considered for the predictive classification purpose. Using linear discriminant analysis, features with high correlation with image classification were selected. Many features, such as correlation, were not selected for the classification process as they were highly correlated with other texture and morphological measurements. Parametric linear discrimination was applied for selected features and the number of correct and misclassified cases was defined for the evaluation of the system performance. Finally, by measuring the sensitivity, specificity, and total accuracy, the discrimination power of the chosen features can be determined. These measures can be calculated using the following formulas:

$$Sensitivity = \frac{TP}{FN+TP}\ 100\ (\%) \tag{8}$$

$$Specificity = \left(100 - \frac{FP}{TN+FP}\ 100 \right)(\%) \tag{9}$$

where *TP*: true positive, *TN*: true negative, *FP*: false positive, and *FN*: false negative.

RESULTS

TEXTURE ANALYSES

The results in Table 2 show that texture is a significant descriptive discriminant for histological images of the colon. The distribution within each group is a multivariate normal distribution and the statistics is estimated from the data by fitting the model to them. All cases are shown to exhibit strong significance ($P < 0.0001$) between normal and malignant tissues samples. Normal images are shown to produce higher values of homogeneity compared to images from cancerous cases. Furthermore, it can be observed that INVDM is inversely related to contrast. As for ASM measurements, it is evident that normal tissues have classes with low values, *i.e.* near the GLCM diagonal. Finally, with regard to entropy, it is clear that normal cases have higher values as it is inversely related to ASM.

MORPHOLOGICAL ANALYSES

Results obtained using morphological analysis presented in Table 3 show that a strong significance ($P < 0.0001$) was observed for the Euler number, NCI, BE, and FD parameters. The distribution within each group is a multivariate normal distribution and the statistics is estimated from the data by fitting the model to them. These parameters are based on the shape/structure of the gland objects (Fig. 2). Elongation and convex area provide less significance as they describe features that could be found in both tissue classes. For example, elongation is described as the ratio between major to minor axes of the region of interest.

COMBINED TEXTURAL AND MORPHOLOGICAL METHODS

Results in Table 4 show that by using four morphological features (Euler number, NCI, elongation and convex area), in combination with three other texture features (entropy, ASM, and homogeneity), 99 out 102 samples could be recognized. The whole dataset is used to specify abnormalities between the cancerous and normal images. This approach has led to 97.1 % accuracy with 98.3 %, and 95.5 %, of sensitivity and specificity, respectively. Although almost all morphological parameters are statistically significant, some measurements were not selected for classification as they were correlated with other features and consequently do not contribute to the discrimination analysis. However, an extra sample was correctly diagnosed when FD, and BE were also combined, leaving one sample from each group wrongly classified. A combined textural and morphological method shows that a total accuracy of 98 % is achieved.
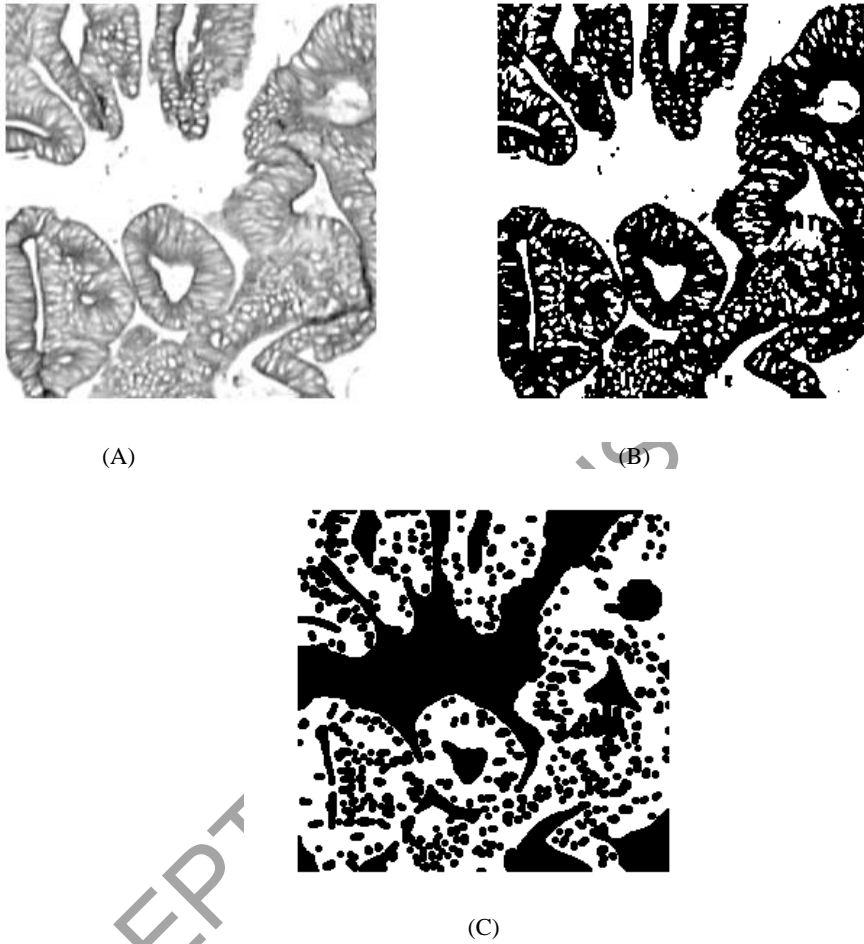
(A)

(B)

(C)

Fig. 3. Applied process to segment the colon tissue samples for Euler numbers measures; (A) Cancer image presenting irregular shape and the glands object are distributed randomly. (B) Thresholds image. (C) Segmented image after open/close morphological operations.
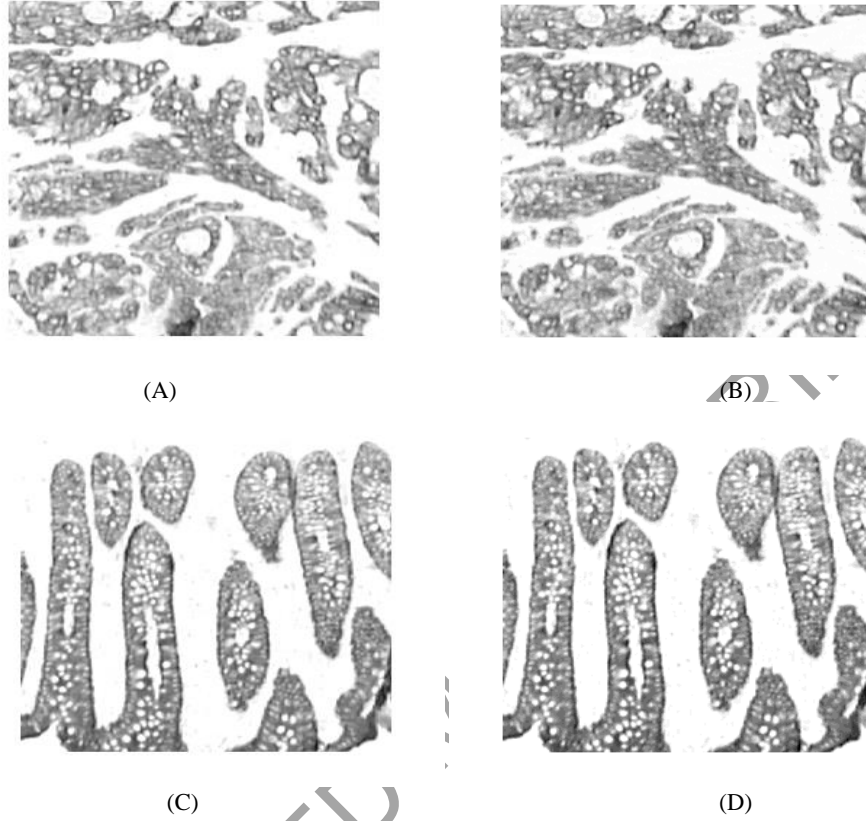
(A)

(B)

(C)

(D)

Fig. 4. Two different samples in different grey-level format. Malignant sample (A) and normal (C) are on 8-bit format while the same samples on (B), and (D) were linearly scaled into 5-bit format (32-grey levels).

Table 3

Statistical evaluation in comparison between normal and colon cancer tissue type for the morphological feature estimated (Mean±standard deviation) [25, 26] with t-test

Texture feature	Normal	Malignant	*P* values
Euler number	12.500±25.353	−29.775±29.291	*P* < 0.0001
Convex area	(3.80±2.46) ×10^{+4}	(5.70±0.986) ×10^{+4}	*P* < 0.01
Nuclear contour index	44.069±35.294	26.431±9.141	*P* < 0.0001
Elongation	1.3587±1.0932	1.410±0.4282	*P* < 0.01
Shape factor (BE)	0.004±0.0034	0.026±0.0214	*P* < 0.0001
Fractal dimension (FD)	1.418±0.0249	1.3508±0.0689	*P* < 0.0001

Table 4

Classification summery of an overall data set using the linear discrimination function. NB. (TP: true positive, TN: true negative, FP: false positive, FN: false negative, SENS: sensitivity, and SPEC: specificity)

Method	TP (%)	TN (%)	FP (%)	FN (%)	SENS (%)	SPEC (%)	Positive predictive value (%)	Negative predictive value (%)	Overall accuracy (%)
Linear discrimination method	57	43	1	1	98.3	97.7	98.3	97.7	98

DISCUSSION

In the past few years, several approaches dealing with histological images were reported [2, 8, 11, 12, 13, 16, 17, 24, 28, 36]. The reported studies have investigated several morphometric, texture, and fractal geometry [14] approaches. Baak [3] reported that an individual feature could rarely completely discriminate between different category types, while combining several features can yield better classification between the groups. Esgiar *et al.* [12] show that the fractal dimension alone achieves only 75.5 % but it has the advantage of increasing the classification ratio for the texture feature from 88.2 % to 94.1 %. In contrast, we show that texture feature can increase the accuracy level for the morphological features based on the shape of tissue glands from 90.2 % [3] to 97.1 %. This paper has shown that the contribution of the fractal dimension combined with the shape factor BE is to increase the accuracy level to 98 %. This classification improvement is a small contribution to that achieved in [11, 12]. This is because self-similarity can only be applied over a limited range, and therefore, it is possibly insufficient to justify the use of the fractal [21, 34]. A better result in terms of the classification ratio has been reported in [24], however, the proposed method had the disadvantage of using huge number of features when low frequency texture measurements of multiresolution color texture were combined with fine second order texture measurements. Their result claims that color was useful to specify abnormalities within the colon cancer dataset. To our knowledge, none of other recent investigations [1, 12, 28, 36] have demonstrated any improvement over our reported results in the classification of colon microscopic images. We noted that none of the approaches alone could give full classification of microscopic colon tissue. Texture and shape are the most powerful descriptors to quantify abnormalities, but considering color texture analysis can be helpful to achieve more improvements.

We should acknowledge some limitations that may has direct effects to our result as following: the results were from a single data set and therefore, our results cannot be extrapolated verbatim to all possible cases; the diagnosis was performed by a single pathologist, thus, invalidated by a second opinion; the possible spurious misclassification errors is due to small resolution image used and maybe because of the use of an un-calibrated image capture device; the small sample size, which effect the accuracy of our model; and we did not validate our model against independent data sets.

In brief, the assessment of histological microscopic images is not a trivial task due to the complexity of such images. An investigation of combining morphological and texture features shows that only two cases from 102 were misclassified.

CONCLUSION

The development of an automated algorithm for precise and reliable decision-making in the discrimination of normal and malignant colon mucosa was proposed. This technique focuses on gland shape and grey level pixel neighborhood. Using grey level co-occurrence method and mathematical morphology, two quantitative feature sets based on texture and morphology, were estimated. These were entropy, ASM, contrast, INVDM, correlation, and homogeneity, representing texture features and Euler number, convex area, NCI, elongation, form factor BE, and FD representing morphological features. Only one case from each group (44 normal, 58 malignant cases) was misclassified. In conclusion, this approach demonstrates a very strong result with an overall accuracy of 98 % for the identification of colon microscopic images. The classification results are limited because they were obtained against an invalidated diagnosis. In addition, further process based on calibration/correction of histological imaged should be considered. Further work of combining color texture analysis with a morphological approach could help to achieve reliable automated image analysis of histological images.

REFERENCES

1. AVNIR, D., O. BIHAM, D. LIDAR, O. MALCAI, Is the geometry of nature fractal?, *Science* (Washington DC), 1998, **279**, 39-40.
2. AZIZ, D.C., R.B. BARATHUR, Quantitation and morphometric analysis of tumors by image analysis, *J. Anal. Biochem.*, 1994, **19,** 120−125.
3. BAAK, J.P.A., *Manual of Quantitative Pathology in Cancer Diagnosis and Prognosis*, Springer Verlag, New York, 1991.
4. BRIGHAM, E., *Fast Fourier Transform and its Applications*, Englewood Cliffs, NJ. Prentice, Hall, 1988.
5. CHEN, C.H., L.F. Pau, P.s.P. Wang, (eds.), *The Handbook of Pattern Recognition and Computer Vision*, 2nd Edition, World Scientific Publishing Co., 1998, pp. 207−248.

6. COSTA, L.da F. R.M. CESAR, J. COSTA, *Shape Analysis and Classification*: *Theory and Practice*, CRC Press, 2000.

7. DAVIS, L.S., Polarograms: a new tool for texture analysis, *Pattern Recognition*, 1981, **13**, 219−223.

8. DEVVI, S., R.H. PARADISA, A. BUSTAMAM, A. PINKIE, Deep learning in image classification using residual network (ResNet) variants for detection of colorectal cancer, *Procedia Computer Science*, 2021, **179**, 423−431.

9. DOUDKINE, A., C. MACAULAY, N. POULIN, B. PALCIC, Nuclear texture measurements in image cytometry, *Pathologica*, 1995, **87,** 286–299.

10. EINSTEIN, A., J. BARBA, P. UNGER, J. GIL, Nuclear diffuseness as a measure of texture: definition and application to the computer-assisted diagnosis of parathyroid adenoma and carcinoma, *J. Microsc.*, 1994, **176,** 158–166.

11. ESGIAR, A.N., R.N.G. NAGUIB, B.S. SHARIF, M.K. BENNETT, A. MURRAY, Automated feature extraction and identification of colon carcinoma, *Anal. Quant. Cytol. Histol.*, 1998, **20**, 297−301.

12. ESGIAR, A.N., R.N.G. NAGUIB, B.S. SHARIF, M.K. BENNETT, A. MURRAY, Fractal analysis in the detection of colonic cancer images**,** *IEEE Trans. Inf. Tec. in Biomedicine*, 2002, **6**, 54−58.

13. FILIPPAS, J., S.A. AMIN, R.N.G. NAGUIB, M.K. BENNETT, *A Distributed System for The Classification of Cancerous and Normal Colonic Mucosa Tissue Images,* Proceeding *of the Second Joint EMBS/BMES Conference***,** 2002, 1120−1121.

14. FILIPPAS, J., H. AROCHENA, S.A. AMIN, R.N.G. NAGUIB, M.K. BENNETT, Comparison of two ai methods for colonic tissue images classification, In: *Proceeding of the 25th Annual International Conference of the IEEE EMBS*, Cancun, Mexico, 2003, 1323-1326.

15. GALLOWAY, M.M., Texture analysis using gray level run lengths, *Comput. Graph Image Process*, 1975, **4,** 172–179.

16. GLASBEY, C.A., G.W. HORGAN, *Image Analysis for Biological Science*s, Chichester, U.K., Wiley, 1994.

17. HAMILTON, P.W., D.C. ALLEN, P.C.H. WATT, C.C. PATTERSON, J.D. BIGGART, Classification of normal colorectal mucosa and adenocarcinoma by morphometry, *Histopathology*, 1987, **11**, 901-911.

18. HAMILTON, P.W., P.H. BARTELS, D. THOMPSON, N.H. ANDERSON, R. MONTIRONI, Automated location of dysplastic fields in colorectal histology using image texture analysis, *J. Pathol.*, 1997, **182**, 68−75.

19. HARALICK, R.M., K. SHANMUGAM, I. DINSTEIN, Textural feature for image classification, *IEEE Trans. Systems Man Cybern.*, 1973, **SMC-3**, 610−621.

20. HARALICK, R.M., Statistical and structural approaches to texture, *Proc. IEEE,* 1979, **67**, 786−804.

21. HARALICK, R.M., R.S. STERNBERG, X. ZHUANG, Image analysis using mathematical morphology*, IEEE Transactions on Pattern Analysis and Machine Intelligence*, PAMI-9, 1987, **4**, 532−550.

22. KRISHNAN, M.M., P. SHAH, A. CHOUDHARY, C. CHAKRABORTY, R.R. PAUL, K.A. RAY, Textural characterization of histological images for oral sub-mucous fibrosis detection, *Tissue Cell*, 2011, **43**(5), 318−330.

23. MARGHANI, K., S. DLAY, B. SHARIF, A. SIMS, Automated morphological analysis approach for classifying colorectal microscopic images, *Proceedings of SPIE − The Int. Soc. Optical Eng. (Intelligent Robots and Computer Vision XXI),* 2003, **5267**, 240−249.

24. MARGHANI, K., S. DLAY, B. SHARIF, A. SIMS, Morphological and texture features for cancers tissues microscopic images, *Proceedings of SPIE − The Int. Soc. Optical Eng.*, 2003, **5032** III, 1757-1764.
25. MARGHANI, K., S. DLAY, A. SIMS, B. SHARIF, Shape analysis and classification in the identification of colon texture images, In: *Recent Advances in Intelligent Systems and Signal Processing*, *Proceedings of the 7th WSEAS International Multiconference CSCC*, 2003, 140−145.
26. OTSU, N.A., Threshold selection method from gray-level histograms, *IEEE Transactions on Systems, Man, and Cybernetics*, 1979, **9**, 62−66.
27. PENTLAND, A.P., Fractal-based description of natural scenes, *IEEE Trans Pattern Anal. Machine Intell.,* **PAMI-6**, 1984, 661–674.
28. PENTLAND, A.P., Fractal-based description of natural scenes, *IEEE Trans. on Pattern Analysis and Machine Intelligence*, 1975, **6**, 661−674.
29. PRESSMAN, N.J., Markovian analysis of cervical cell images, *J. Histochem. Cytochem.*, 1976, **24,** 138–144.
30. RATHORE, S., M. HUSSAIN, M.A. IFTIKHAR, A. JALIL, Novel structural descriptors for automated colon cancer detection and grading, *Journal of Computer Methods and Programs in Biomedicine*, 2015, **121**, 92−108.
31. SAIMA, R., H. MUTAWARRA, K. ASIFULLAH, Automated colon cancer detection using hybrid of novel geometric features and some traditional features, *Computers in Biology and Medicine*, 2015, **65**, 279−296.
32. SERRA, J., *Image Analysis and Mathematical Morphology*, vol. 1, Academic Press Inc., London, 1982.
33. SHUTTLEWORTH, J.K., G.A. TODMAN, G.N.R. NAGUIB, M.B. NEWMAN, Multiresolution colour texture analysis for classifying colon cancer images, In: *Proc. of the 2002 IEEE Canadian Conference on Electrical & Computer Engineering*, 2002, **2**, 1118−1119.
34. TENGUAM, J.J., G.B. ROZENDO, G.F. ROBERTO, M.Z. DO NASCIMENTO, A.S. MARTINS, L.A. NEVES, Multidimensional and multiscale Higuchi dimension for the analysis of colorectal histological images, *2020 IEEE International Conference on Bioinformatics and Biomedicine (BIBM)*, 2020, **1**, 2833−2839
35. THIRAN, J.P., B. MMCQ, Morphological feature extraction for the classification of digital images of cancerous tissues, *IEEE Trans. on Biomedical Eng*., 1996, **43**(10), 1011−1019.
36. WEIBEL, E.R., *Stereological Methods: Practical Methods for Biological Morphometry*, vol. 1, Academic Press, London, 1979.